# Reports

## Astronomical Theory of Climatic Change: Support from New Guinea

Abstract. *Radiocarbon and thorium-230 dates of uplifted coral reef terraces on New Guinea appear to support theories of glaciation which utilize Milankovitch cycles as a controlling trigger mechanism. In addition to high sealevel stands recognized by other workers, the New Guinea data clearly indicate a marine transgression between 50,000 and 35,000 years before the present. A eustatic sea level curve reconstructed from field observations and radiometric dates shows a close correlation with temperature fluctuations in high latitudes as predicted by astronomical data.*

The astronomical theory of glaciation, first proposed in comprehensive form by Milankovitch (*1*) and based on perturbations in the earth's orbit with concomitant variations of solar insolation, has received increasing attention in recent years because it is tied to a rigid time scale and hence can be tested by absolute dating of certain paleoclimatic indicators. From the outset, a successful test by absolute dating requires a precision which is better than 10,000 years (half the precessional cycle of the earth's axis) and a range which covers as many cycles as possible. Under optimum conditions, some of the newly developed dating techniques that involve intermediate members of the uranium decay series fulfill these conditions, at least for the last 200,000 years. By using such techniques, persuasive correlations between the Milankovitch radiation curve and variations in the ocean surface temperature (*2*), as well as eustatically controlled high sea-level stands (*3, 4*) have been obtained.

In this report we attempt to reconstruct a sea level curve for the last 200,000 years, interpreted from uplifted coral reefs in New Guinea and calibrated by $C^{14}$ and $Th^{230}$ dates of unrecrystallized corals and *Tridacna* clam shells. This sea level curve appears to support theories of glaciation which utilize Milankovitch cycles as a controlling trigger mechanism (*5, 6*).

An extensive flight of uplifted coral reef terraces occurs along 100 km of the northern flank of the Huon Peninsula, northeast New Guinea (Fig. 1, inset map). Over 20 uplifted reefs of a wide range of widths and thicknesses make a complex flight of terraces rising to over 700 m above sea level in the east and center of the area. Elevation of every terrace varies laterally, for example, a particular terrace falls from a 400-m altitude in the center of the area to 33 m at the point where it fades out, some 60 km to the northwest, reflecting a differential in uplift rates of over 10:1. The zone of greatest uplift rates has migrated through time, for while some terraces tend to converge laterally in a westward direction, others converge to the east. The terraces overlie conglomerates and Pliocene limestones and marine tuffaceous graywackes which constitute the bulk of the Huon Peninsula ranges; a complete description appears elsewhere (*7*).

The series of offlapping reefs includes both fringing reefs and ancient barrier-reef lagoons. If one assumes that a barrier reef develops when a rising sea overtakes the land, transgressions may be recognized. Maximum rates of uplift are around 3 mm/year (shown by the age estimates below); therefore lagoons will form only if the rates of sea level rise are of this order, or more. The postglacial transgression appears to have had a mean rate of 7 mm/year (*8*), and hence transgressions recognized in

Table 1. Radiometric ages for corals and *Tridacna* shells from uplifted coral reef terraces on Huon Peninsula, New Guinea. Errors are based on counting statistics. C, coral; T, *Tridacna gigas*.

| Sample No. | Material | Uranium (ppm) | $U^{234}:U^{238}$ | $Th^{230}:U^{234}$ | $Th^{230}$ age ($\times 10^3$ yr) | $C^{14}$ age ($\times 10^3$ yr) |
|---|---|---|---|---|---|---|
| | | | *Reef complex I* | | | |
| ANU 165 | C | 2.51 ± 0.05 | 1.12 ± 0.01 | 0.05 ± 0.005 | 6 ± 1 | 6.7 ± 0.06† |
| ANU 153* | T | 0.056 ± .005 | 1.27 ± .09 | .06 ± .005 | | 6.8 ± .1† |
| | | | *Reef complex II* | | | |
| ANU 156 | T | | | | | 29.3 ± .9 |
| | | | *Reef complex III* | | | |
| ANU 150* | T | .11 ± .003 | 1.14 ± .03 | .35 ± .02 | 46 ± 3 | 30.9 ± .9 |
| ANU 116* | T | .24 ± .01 | 1.14 ± .07 | .27 ± .03 | 34 ± 4 | 35.8 ± 1.5 |
| AUN 117* | T | .13 ± .003 | 1.13 ± .03 | .19 ± .01 | 23 ± 2 | 35.4 ± 1.3 |
| NG 600 | C | 2.48 ± .04 | 1.13 ± .01 | .39 ± .02 | 53 ± 3 | |
| NG 601 | C | 2.30 ± .04 | 1.12 ± .01 | .37 ± .02 | 49 ± 3 | |
| | | | *Reef complex IV* | | | |
| NG 623 | T | 0.228 ± .004 | 1.12 ± .02 | .43 ± .03 | 60 ± 6 | |
| NG 625 | T | .36 ± .08 | 1.10 ± .02 | .50 ± .02 | 74 ± 4 | |
| | | | *Reef complex V* | | | |
| NG 618 | C | 2.49 ± .06 | 1.11 ± .01 | .67 ± .02 | 116 ± 7 | |
| NG 618 | C | 2.41 ± .05 | 1.11 ± .01 | .68 ± .02 | 119 ± 7 | |
| NG 616 | C | 2.15 ± .04 | 1.10 ± .01 | .74 ± .03 | 140 ± 10 | |
| NG 616 | C | 2.07 ± .04 | 1.12 ± .02 | .72 ± .03 | 133 ± 10 | |
| | | | *Reef complex VI* | | | |
| NG 610 | C | 2.86 ± .06 | 1.10 ± .01 | .85 ± .03 | 190 ± 17 | |
| NG 610 | C | 2.71 ± .05 | 1.09 ± .01 | .83 ± .03 | 180 ± 15 | |
| NG 615 | T | 0.65 ± .01 | 1.20 ± .02 | .56 ± .03 | 87 ± 7 | |
| | | | *Reef complex VII* | | | |
| NG 398 | C | 2.75 ± .06 | 1.09 ± .02 | .93 ± .04 | ≧ 250 | |
| NG 430 | C | 2.59 ± .05 | 1.10 ± .01 | .89 ± .04 | 215 ± 30 | |
| NG 604 | C | 2.59 ± .05 | 1.10 ± .01 | .91 ± .03 | ≧ 230 | |
| NG 608 | C | 2.44 ± .05 | 1.10 ± .01 | .96 ± .04 | > 250 | |
| NG 609 | C | 2.42 ± .04 | 1.08 ± .01 | .88 ± .04 | 210 ± 30 | |
| | | | *Reef complex VIII* | | | |
| NG 605 | C | 2.31 ± .06 | 1.05 ± .02 | .98 ± .04 | > 250 | |
| NG 606 | C | 2.21 ± .04 | 1.09 ± .01 | .97 ± .04 | > 250 | |
| | | | *Early Pleistocene* | | | |
| NG 405 | C | 2.22 ± .06 | 0.96 ± .02 | 1.03 ± .04 | > 250 | |

* Sample contains $Th^{232}$ and is corrected for nonradiogenic $Th^{230}$ assuming early addition of thorium isotopes with $Th^{230}:Th^{232} = 1.2$ (*14*). † In the text these ages are reduced to 6300 years because dated modern corals and shells (*9*) from the same area indicate $C^{14}$ dilution by upwelling seawater.

the reef succession are inferred to be of glacio-eustatic origin. Broad fringing reefs are assumed to have formed when rising land and sea have kept pace with one another, and steep descents from one terrace to another developed when the land rose rapidly relative to the sea —a condition most likely during a glacio-eustatic regression. Regressions could be separated from sea-level still-stands near the western end of the terrace flight, where the rate of uplift has been least rapid. Figure 1 shows changes in sea level relative to those of the land, interpreted according to these principles, for two typical sections.

Twelve sections similarly interpreted consistently agree as to the number of transgressions and their points of commencement (*7*), but these data cannot be converted into a sea level curve without fixing the ages of some of the reefs.

Corals and *Tridacna gigas* shells were collected *in situ* from each reef (sample locations in Fig. 1) and dated by the $C^{14}$ or $Th^{230}$ methods, or both (Table 1). The $C^{14}$ dates, together with supporting isotopic data, are published elsewhere (*9*); a complete discussion of the $Th^{230}$ method of dating marine carbonates can be found in the literature (*10*). Uranium and thorium isotopes were measured by alpha-spectrometry, with the use of $U^{232}$ and $Th^{234}$ yield tracers (*11*). Both the $C^{14}$ and $Th^{230}$ methods require unrecrystallized material. Since both corals and *Tridacna* deposit their skeletons as aragonite, the onset of recrystallization to calcite can be detected by x-ray diffraction. Only samples containing less than 5 percent calcite were used in this study.

In general, corals appear more reliable for $Th^{230}$ dating than mollusks do (*10*) and have been used wherever possible. Because the original uranium content in shells of living mollusks is very low—less than 1 part per million (ppm) (*12*)—their $Th^{230}$ ages are very susceptible to large errors due to environmental contamination by uranium (*13*) and nonradiogenic $Th^{230}$ (*14*). The isotopic data from the fossil corals (see Table 1), on the other hand, are consistent with the assumption that the uranium is primarily derived from sea-water, without further contamination by either uranium or thorium. On those terraces where unrecrystallized corals could not be found, *Tridacna* shells, which appear more resistant to recrystallization, were used instead. Two shell samples, NG 623 and NG 625, are judged reliable. As in the fossil corals, the low $U^{234}$:$U^{238}$ ratios and the absence of $Th^{232}$ suggest that these two shells have remained largely unaf-

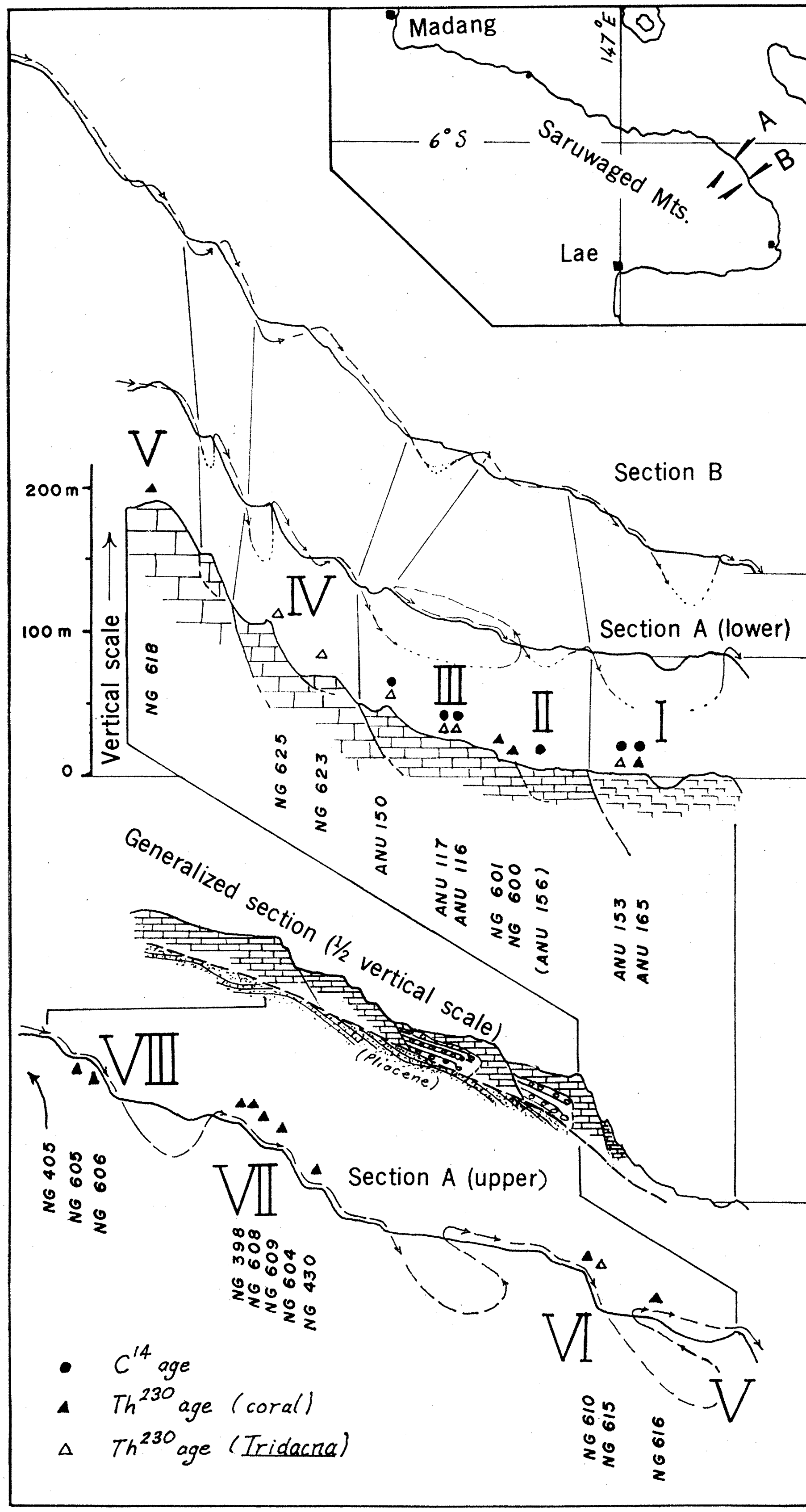


Fig. 1. Two typical sections across northeast New Guinea terraces; location shown at top right. Fine broken line with arrow marks shows movement of strand line, inferred from reef stratigraphy, during emergence of the land. Roman numerals refer to separate reef complexes (see Table 1). Position of dated samples shown.

fected by postdepositional contamination.

The ages listed in Table 1 for the different reef complexes, together with their stratigraphic relationships (Fig. 1), suggest periods of relatively high eustatic sea level between 190,000 and 180,000 years B.P., between 140,000 and 118,000 years B.P., close to 74,000 years B.P., and between 50,000 and 35,000 years B.P., as well as the present period of high sea level commencing about 6000 years ago. Most of these sea level maximums have been reported independently from other continents (*3, 4, 15*).

An attempt was made to reconstruct a sea level curve as follows. The 118,000-year age of sample NG 618 (Table 1 and Fig. 1) dates the termination of a period of relatively stable sea level which commenced earlier than 140,000 years ago, as indicated by sample NG 616. Data accumulated in recent years suggest that about 120,000 years ago the sea stood between 2 and 10 m higher than it does at present (*15*). Subtracting this from the height above sea level of sample NG 616 (which is from a lagoon barrier reef) gives the uplift of a hypothetical strand line which formed at present sea level 120,000 years ago. The heights above sea level of the dated horizons, measured on the traverse including sample NG 616 (at point *D*, Fig. 2), can now be plotted versus age on the same graph, and an uplift curve (lines *CD* and *CE*, *ED* in Fig. 2) can be constructed. The

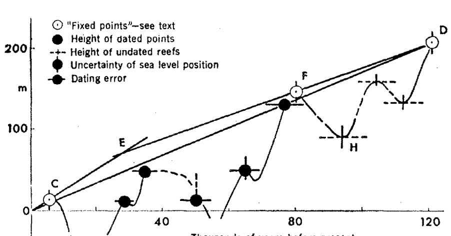


Fig. 2. Method of reconstructing sea level curve. For a particular section (for example, *A*, Fig. 1), mark in the height to which a reference strand line has been lifted—for example, point *D*. (A reference strand line is one for which world data give a good specification of both age and sea level relative to the present.) Plot in dated reefs at their appropriate heights and undated reefs at their probable positions, adding error bars. Other "fixed" points (*C* and *F*) indicate that uplift is unlikely to have been uniform, and limiting curves *CE, ED* are drawn. Vertical intervals from these to dated reef points give depressions of sea level relative to the present; the final curve is the mean of reconstructions of 12 sections.

pattern of deformation of the terraces implies that uplift has not been uniform through time along any particular traverse line, hence the uniform uplift curve *CD* is unrealistic. Segments of the uplift curve *CE* and *ED* are constructed from age data of particular sea levels identified elsewhere, that is, 80,000 years B.P., sea level within −13 and −16 m of the present level (*4*); 6300 years B.P. sea level within −5 and −12 m of present (*8*). In addition to the uncertainty associated with these levels, there is also an error associated with placing correctly in time the undated parts of the reef succession, for example, the sea level low, recognized stratigraphically and marked *H* in Fig. 2. In spite of these factors the curves derived from all traverses are in consistent agreement (*7*) and from these data the generalized sea level curve in Fig. 3C is derived.

Let us now compare this with the Milankovitch radiation curve. It has been customary in the past to express this curve in terms of equivalent latitude (*1*) or arbitrary radiation units (*3, 4*) as shown in Fig. 3A. However, such radiation curves make no allowance for lateral heat exchange and thus may be unrealistic. A quantitative evaluation of the effect of these insolation changes on the actual surface temperature field in the Northern Hemisphere has recently been presented by Shaw and Donn (*16*), based on meteorological data and with the use of a thermodynamic model which incorporates horizontal heat transport. Three curves have been constructed from their published data for the mean summer temperature variations at 65°N, 45°N, and 25°N during the last 200,000 years (Fig. 3B). These curves show, in effect, the relative importance of precession and tilt at the different latitudes.

The actual variations of temperature predicted by the Milankovitch model are too small to directly account for known changes of temperature in the Pleistocene (*16*). However, we are considering theories which invoke the insolation minimums as a mere triggering mechanism for an initially temperature-sensitive, but later self-amplifying, ocean-ice system (*5, 6, 17*). An important consequence of such models is the appearance of a time lag between primary cause (change in insolation) and ultimate effect (change in volume of ice). Fluctuations in sea level should exhibit the same time lag as the total ice volume with respect to its primary cause. It is uncertain whether interglacial and interstadial high sea levels will bear the same lag relationship to insolation minimums, because of the possible involvement of the Arctic floating ice sheet (*17*). With respect to low sea levels, it appears that the last major minimum was 15,000 to 20,000 years ago (*8*), whereas the corresponding insolation minimum was 22,000 years ago (Fig. 3A), giving a response time of 2000 to 7000 years. A lag of this magnitude appears consistently between insolation minimums and low points on the sea level curve (Fig. 3). Similarly, high sea-level stands appear to display a systematic covariance with insolation maximums, although a cause and effect relationship as suggested by Broecker and co-workers (*3, 4*) is still open to dispute for reasons given above. In view of uncertainties introduced by the tectonic factor and by the inherent analytical errors of dating, the agreement between the sea level fluctuations and their postulated primary cause is surprisingly good. Because of the interplay of isostatic and meteorologic factors in the ice-climate system (*5*), one would not expect a close correspondence in detailed form of the two curves.

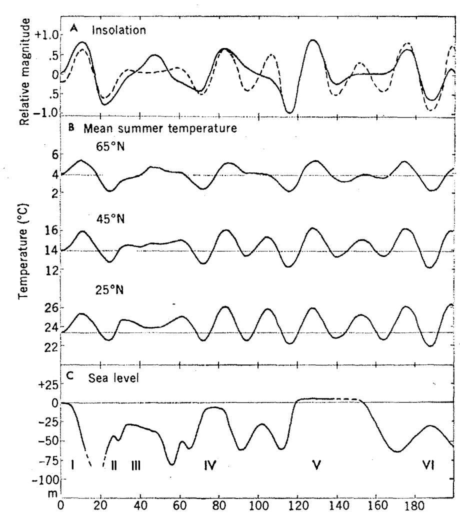


Fig. 3. (A) Summer insolation curves for the Northern Hemisphere showing predominant effect of tilt (solid line) as compared to that of precession (dashed line) [Redrawn from Broecker (*3*)]. (B) Variation of mean summer surface temperature at different latitudes in the Northern Hemisphere as calculated by Shaw and Donn (*16*), using astronomical and meteorological data. The horizontal lines show present-day temperatures for comparison. (C) Eustatic sea level fluctuations as reconstructed from field observations and supported by radiometric dates (see text). The horizontal line indicates the present sea level. Roman numerals refer to dated reef complexes (see Table 1 and Fig. 1).

The customary insolation curve at 65°N (Fig. 3A, solid line) shows an insolation maximum at around 48,000 years B.P. Failure to find evidence for a high sea-level stand corresponding to this insolation maximum compelled Broecker (*3*) to give the precession effect relatively more weight than the tilt effect, implying that the temperature-sensitive latitudes in the ice-climate system are farther south than 65°N. With this weighting the prominent insolation maximum at 48,000 years is suppressed, while at the same time a new and distinct insolation high appears at 105,000 years (Fig. 3A, dashed line). This argument is strengthened by the Barbados data (*4*) which show some evidence for a separate high sea stand at about 102,000 years B.P. We were unable to directly date such a high sea-level stand in New Guinea, although the field evidence indicates a distinct transgression between the "80,000"- and "125,000"-year sea stands which almost certainly corresponds to the "105,000"-year stand on Barbados. However, our results from New Guinea show quite clearly that the sea stood relatively high between 50,000 and 35,000 years ago. A similar high sea stand between about 60,000 and 40,000 years ago has been reported from Kikai-Jima in the Ryukyu Islands (*18*). Failure to identify this high sea stand on Barbados can be explained by the lower uplift rate of Barbados [~ 0.3 mm/year (*4*)] as compared to that of New Guinea (1 to 3 mm/year), and especially if uplift of Barbados was nonuniform rather than uniform as assumed.

The New Guinea data independently confirm, either directly or indirectly, each high sea-level stand identified on Barbados for the last 230,000 years, thus supporting the idea that these sea level stands are indeed eustatic. The 50,000- to 35,000-year transgression found on New Guinea improves the close correlation of eustatic sea level fluctuations with predicted insolation changes in the Northern Hemisphere for the last 200,000 years. This can hardly be a coincidence and strongly supports theories of glaciation which utilize insolation changes as a controlling trigger mechanism.

H. HERBERT VEEH
*Department of Geophysics and Geochemistry, Australian National University, Canberra, A.C.T.*
JOHN CHAPPELL
*Department of Geography, Australian National University*

**References and Notes**

1. M. Milankovitch, in *Handbuch der Geophysik*, W. Koppen and R. Geiger, Eds. (Borntraeger, Berlin, 1938), vol. 9, p. 593.
2. C. Emiliani, *J. Geol.* **74**, 109 (1966).
3. W. S. Broecker, *Science* **151**, 299 (1966).
4. ———, D. L. Thurber, J. Goddard, T.-L. Ku, R. K. Matthews, K. J. Mesolella, *ibid.* **159**, 297 (1968); K. J. Mesolella, R. K. Matthews, W. S. Broecker, D. L. Thurber, *J. Geol.* **77**, 250 (1969).
5. C. Emiliani and J. Geiss, *Geol. Rundschau* **46**, 576 (1959).
6. J. M. A. Chappell, *Nature* **219**, 36 (1968).
7. ———, thesis, Australian National University, in preparation.
8. F. P. Shepard, *Z. Geomorphol.* Supplbd. **3**, 30 (1961); J. R. Curray, in *The Quaternary of the United States*, H. E. Wright and D. G. Frey, Eds. (Princeton Univ. Press, Princeton, N.J., 1965), p. 723; J. D. Milliman and K. O. Emery, *Science* **162**, 1121 (1968).
9. H. A. Polach, J. Chappell, J. F. Lovering, *Radiocarbon* **11**, 245 (1969).
10. D. L. Thurber, W. S. Broecker, R. L. Blanchard, H. A. Potratz, *Science* **149**, 55 (1965).
11. The alpha-spectrometer used in this study consisted of an Oak Ridge Technical Enterprises Corporation solid state detector and ORTEC 101/201 low-noise amplifier system, connected to a Reduction Instrument Development Laboratory 200-channel pulse height analyzer. The beta activity of the $Th^{234}$ tracer was measured with an end-window Geiger counter.
12. M. Tatsumoto and E. D. Goldberg, *Geochim. Cosmochim. Acta* **17**, 201 (1959); W. S. Broecker, *J. Geophys. Res.* **68**, 2817 (1963); R. L. Blanchard, M. H. Cheng, H. A. Potratz, *ibid.* **72**, 4745 (1967).
13. The uranium content in a modern specimen of *Tridacna gigas* from this same New Guinea coast was less than 0.002 ppm; therefore, almost the entire uranium content measured in fossil shells of this species appears to be of secondary origin. Unless this secondary uranium enters the shell carbonate shortly after the death of the organism, serious errors in age result—thus the measured age of sample NG 615 is too young by comparison with the ages of apparently reliable adjacent corals. The abnormally high $U^{234}:U^{238}$ ratio in this sample indicates isotopic exchange with nonmarine waters where the $U^{234}:U^{238}$ ratio frequently is higher than in seawater [D. L. Thurber, *J. Geophys. Res.* **67**, 4518 (1962)].
14. Correction for nonradiogenic $Th^{230}$ was required for samples ANU 116, ANU 117, and ANU 150 which contained 0.03, 0.04, and 0.02 ppm of $Th^{230}$, respectively. The $Th^{230}:Th^{232}$ ratio of 1.2 in this correction was estimated in a similar manner as suggested by A. Kaufman and W. S. Broecker [*J. Geophys. Res.* **70**, 4039 (1965)], using the $Th^{232}$ content (0.03 ppm) and known $C^{14}$ age of sample ANU 153. This correction introduces an additional uncertainty, because the $Th^{230}:Th^{232}$ ratio may vary and because the time of addition of these isotopes to the shell carbonate has to be assumed.
15. J. K. Osmond, J. R. Carpenter, H. L. Windom, *J. Geophys. Res.* **70**, 1843 (1965); W. S. Broecker and D. L. Thurber, *Science* **149**, 58 (1965); H. H. Veeh, *J. Geophys. Res.* **71**, 3379 (1966).
16. D. M. Shaw and W. L. Donn, *Science* **162**, 1270 (1968).
17. M. Ewing and W. L. Donn, *ibid.* **127**, 1159 (1958); W. L. Donn and D. M. Shaw, *J. Geophys. Res.* **71**, 1087 (1966).
18. K. Komura and M. Sakanoue, *Sci. Rep. Kanzawa Univ.* **12**, 21 (1967).

5 September 1969

## Polywater: Methods for Identifying Polywater Columns and Evidence for Ordered Growth

Abstract. *The refractive indices of polywater columns in glass capillaries have been rapidly and accurately measured with an interference microscope. Polywater has been detected by this method in both quartz and Vycor glass capillaries. A comparison of refractive index measurements with measurements of optical anisotropy indicates that polywater initially condenses with an ordered structure.*

Considerable interest has developed recently in the preparation and properties of polywater (*1*), a form of water which has properties quite different from those normally associated with liquid water. We have applied two practical methods of measuring refractive index to the problem of identifying polywater columns in capillaries. The methods are rapid and simple and make use of an interference microscope. Earlier methods of identifying polywater have required the removal of some of the polywater from the capillary (*1, 2*), or use of an uncommon measuring apparatus (*1, 3*), or a minimum column length of 2 to 3 mm (*4*). In contrast, the methods for measuring refractive index described here will detect even small amounts of polywater and measurements can be made directly on the polywater-containing capillaries as they result from the preparation. Moreover, one can use measurements of refractive index and optical anisotropy to draw conclusions about the growth of polywater molecules in the capillary.

Deryagin *et al.* (*3*) identified columns of polywater by measuring the refractive index $\eta$; their method is based on the fact that the liquid filling the bore of the capillary forms a cylindrical lens. The refractive index is obtained by measuring the difference in focal length between the empty and liquid-filled capillary and then referring to a calibration curve determined empirically from measurements of liquids of known $\eta$. Using this method, Deryagin *et al.* measured refractive indices of polywater in the range from 1.335 to 1.5. By comparing polywater with liquids of known refractive index, Lippincott *et al.* (*1*) found that a specimen of polywater had a refractive index of 1.48. Willis *et al.* (*5*) reported that the portion of a column of poly-